Available online at www.sciencedirect.com
SCIENCE DIRECT®
Journal of Nuclear Materials 346 (2005) 109–119
journal of nuclear materials
www.elsevier.com/locate/jnucmat

The effect of Zircaloy-4 substrate surface condition on the adhesion strength and corrosion of SiC coatings

Y. Al-Olayyan [a], G.E. Fuchs [a,*], R. Baney [a], J. Tulenko [b]

[a] Materials Science and Engineering Department, University of Florida, P.O. Box 116400, Gainesville, FL 32611-6400, USA
[b] Nuclear and Radiological Engineering, University of Florida, P.O. Box 118300, Gainesville, FL 32611-8300, USA

Received 15 June 2004; accepted 11 May 2005

Abstract

Chemical vapor deposition (CVD) coatings of silicon carbide were deposited on various Zircaloy-4 substrates having different surface preparations to increase the corrosion resistance. The effects of several different surface treatments of the Zircaloy-4 substrate, such as surface roughness, the presence of interlayer, and pickling, on the adhesion and corrosion resistance of the SiC coatings have been evaluated using a scratch test method, electrochemical impedance spectroscopy and scanning electron microscopy. The scratch test was found to be a good tool for qualitative measurement of adhesion strength of thin coating films. Higher adhesion strengths were obtained for a moderate level of substrate roughness and the corrosion resistance of these films was closely related with the adhesion of the film on the substrate, as measured by impedance.

1. Introduction

High burn-up of pressurized water reactors (PWR's) is limited by corrosion of the Zircaloy fuel cladding. The purpose of this project was to explore the possibility of depositing thin layers of ceramics on the cladding to enhance the corrosion resistance [1].

Silicon carbide has a blend of desirable properties including resistance to corrosive environments at high temperatures, a large band gap, low density, good mechanical behavior, and high thermal stability [2–5]. Silicon carbide coatings have the potential to offer excellent resistance to oxidation and hydriding in Zircaloy cladding for PWR reactors. The most appropriate way to prepare SiC coatings for this proposed application, is by chemical vapor deposition (CVD). CVD coatings are typically deposited via the use of Si–C–H–Cl-based systems. Methyltrichlorosilane, CH_3SiCl_3 (MTS), is often used as a precursor due to its ability to be decomposed at moderate temperatures and because of its relatively low cost [6].

The corrosion performance of ceramic coatings, such as SiC, Si_3N_4 and CrN, has been determined for a number of coating variables. These variables include surface continuity and uniformity, coating defects, adhesion, and substrate roughness [7–11].

Intrinsic defects, such as crack or pores, formed during the deposition process can be particularly detrimental to coating performance in corrosive environments. Galvanic or crevice attack is a common form of degradation of ceramic coated metals, since a

* Corresponding author. Tel.: +1 352 846 3317; fax: +1 352 392 7219.
E-mail address: gfuch@mse.ufl.edu (G.E. Fuchs).

0022-3115/$ - see front matter © 2005 Elsevier B.V. All rights reserved.
doi:10.1016/j.jnucmat.2005.05.016

difference in corrosion potential between metal and coating material exists at the coating/substrate interface in through-coating defects. However, it is possible to enhance the corrosion performance of ceramic coatings by improving adhesion [7,8]. Several acceptable techniques have been proposed to increase the adhesion. The use of inorganic films frequently induces cracking, debonding, or delamination of films from intrinsic compressive or tensile stresses. Common methods used to enhance adhesion include roughening the surface [12–14], ion implantation [13,15–19] and use of a chemically compatible stress-relaxing interlayer [20–22] that has an intermediate thermal-expansion coefficient.

Quantitative determination of the adhesion between coatings (or films) and their substrates is very important. Furthermore, scientific investigation into the nature of coating–substrate adhesion and the development of methods to improve adhesion require the accurate and meaningful measurement of coating adhesion. One of the most popular methods of testing adhesion strength of thin films is the scratch test. Scratch testing has long been used to assess the adhesion of thin hard coatings and is a useful tool for coating development and quality assurance [14,15,21,23–26]. The scratch-test method consists [24] of the generation of scratches with a spherical stylus (generally a Rockwell C diamond tip, with a tip radius of 200 μm) which is drawn with progressive loading at a constant speed across the coating surface to be tested. The critical load (L_c) is defined as the smallest load at which a recognizable failure occurs.

The critical loads depend on the mechanical strength (adhesion, cohesion) of a coating–substrate composite and also on several other parameter [23]. Some of the parameters are directly related to the test itself, while others are related to the coating–substrate system. The test specific parameters of the scratch test include loading rate, scratching speed, and indenter tip radius and indenter material. The coating–substrate specific parameters include substrate hardness and roughness, coating hardness and roughness, coating thickness, friction coefficient between coating and indenter and, internal stresses in the coating.

Usually, highly adherent coatings produce a corrosion protective barrier (e.g., [27]). The study attempts to elucidate the effect of substrate surface treatments and adhesion strength on the corrosion properties of PACVD (plasma assisted chemical vapor deposition) SiC films on Zircaloy-4 substrates. Scratch tests, SEM and impedance tests were used for this evaluation.

2. Experimental

Zirconium alloy (Zircaloy-4) samples were used as substrates. These alloys were forged in the beta region of the equilibrium phase diagram, then solution treated at about 1065 °C and water quenched. Subsequent hot working and heat treating was done in the alpha region (below 790 °C) to preserve the fine, uniform distribution of intermetallic compounds that result from solution treatment and quenching. The samples were cut by EDM (electric discharge machine) to 16 mm diameter × 1 mm thick disks. Thirty five samples were prepared with different surface preparations for PA CVD (1 μm thick) SiC coating. A total of five samples for each of the seven different substrate surface conditions were prepared. All of the samples were ultrasonically cleaned in acetone after each preparation step. Some of the Zircaloy samples were ground to produce varying surfaces finishes. The Zircaloy samples were placed on aluminum samples holders using thermal glue and then wet ground, starting with 240 grit SiC grinding paper. Finer surface finishes were obtained by using finer grit SiC grinding papers (i.e., 400 grit and 600 grit). All polishing was performed by hand. After polishing, all samples were again cleaned in an ultrasonic acetone bath. Some of the samples polished with the 240 grit SiC grinding paper were also given additional surface treatments. One group of samples were pickled with a mixture of 25–50% nitric acid, 2–5% hydrofluoric acid and water and another group was pre-oxidized at 1200 °C for 10 min and air cooled. An additional group of samples polished with 600 grit SiC grinding paper were also carbon coated (5–20 nm thick).

The Zircaloy substrate surface conditions are summarized below:

A. As-received.
B. 600 grit polishing.
C. 240 grit polishing.
D. 240 grit polishing followed by pickling with 25–50% nitric acid (70% vol), 2–5% hydrofluoric acid (49% vol) and water.
E. Grit blasted (grit 40–60 by glass beads).
F. Pre-oxidized (polished to 240 grit, heated to 1200 °C for 10 mins and air cooled).
G. Carbon coated (50–200 Å thick) (polished to 600 grit and ultrasonically cleaned before carbon coating).

The silicon carbide coatings were prepared by MER (Materials and Electrochemical Research Corporation, Tucson, Arizona), using their proprietary low temperature DC-pulsed plasma enhanced chemical vapor deposition (PE-CVD) technique. The temperature of the substrate during deposition was approximately 360–375 °C. The coating film was 1 μm thick and determined to be amorphous by XRD. Typically, the coatings had 10–20% thickness variations, particularly near the specimen edges. The oxidized samples were reported by MER to be difficult to coat, and some of the oxide

Table 1
Test conditions for scratch analysis for all samples (0–15 N) and for selected tests at lower loads (0–3 N)

Loading range	0–15 N	0–3 N
Loading rate, dL/dt (N/min)	15	3
Scratch length (mm)	3	3
Scratching speed, dx/dt (mm/min)	3	3
Acoustic emission sensitivity, S_A	9	9
Indenter (μm)	200	20

may have been removed during coating. After coating, all samples were again cleaned in an ultrasonic acetone bath.

Surface roughness measurements were made on the Zircaloy samples before and after coating using a Wyko NT1000, in order to quantify the roughness effects of the substrate surface/condition on the coating surface roughness. The surface roughness of each sample were based on measurements taken in 3–5 areas, approximately $100\ \mu m \times 200\ \mu m$ in size, and averaged. Scratch-tests were performed at Micro-Photonics (Irvine, CA) on a Micro Scratch Tester (MST) by generating 3–4 scratches on each coated sample using a spherical Rockwell C diamond stylus with a tip radius of 200 μm. The loading range for this testing was 0–15 N. The stylus was drawn at a constant speed across the coating surfaces. The test parameters are shown in Table 1. To insure that accurate measurements of coating adherence were obtained, scratch testing was repeated on selected samples at lower loads (0–3 N) using a finer stylus (20 μm). The critical load was determined by tangential force recording which enables the force fluctuations along the scratch to be followed and also by acoustic emission (AE) detection of elastic waves generated as a result of formation and propagation of microcracks. In order to eliminate any potential for errors, the scratch testing was performed in a random orientation relationship with the polishing/grinding directions on each sample. Although three (3) parallel scratch tests were usually performed on each sample, the remaining tests were performed at varying angles on all samples.

The corrosion protective properties of PE-CVD SiC coatings on six different Zircaloy-4 substrates were characterized by electrochemical impedance spectroscopy (EIS). The measurements were conducted in a 0.001 M HF/1 M HCl/1 M HNO_3 solution at room temperature. Solutions were purged with high-purity Ar gas for 2 h prior to the impedance test. Two high-purity graphite rods were used as counter-electrodes. The reference electrode was a saturated calomel electrode (SCE, 0.241 vs. SHE). The EIS measurements were made using a Gamry PC4 potentiostat and frequency analyzer (FRA). Impedance spectra were measured over the frequency range 0.01–1 000 000 Hz with 5 mV amplitude.

3. Results and discussion

The adhesion surface roughness test for the samples surface before and after coating was determined by profilometry. Roughness results for all samples are summarized in Table 2. The value, R_a, is the arithmetic mean roughness value, which is the average value of all absolute vertical distances of the roughness profile from the center line within the measuring length. Note that there is not a clear relationship between the measured surface roughness of the samples before and after coating. For example, the surface roughness decreased to almost a half after coating for the 240 grit surfaces, but increases for the 600 grit samples and for the as-received surfaces. These large differences of roughness before and after coating suggest that the conformality of the coating was not very high and the thickness of the film at peaks and valleys is different. Roughness of the pre-oxidized sample also increased to twice its original value (600 grit) after oxidation and coating. However, this increase could be attributed to the rough and thick oxide layer.

Secondary and backscattered electron SEM images were obtained for all coated samples. The secondary electron SEM imaging exhibited topographical features, such as scratches or cracks. Backscattered electron SEM images identify compositional differences, particularly if cracks that propagated to the base metal were present. Although significant scratches were seen (Fig. 1) on all coating surfaces, which were caused by grinding the substrate before coating, the backscattered images do not show a similar morphology. Therefore, these scratches do not reach the substrate.

In the as-received substrate, the scratches on the surface of the film were non-uniform (Fig. 2(a)) because the substrate was not polished prior to coating. The film on grit-blasted Zircaloy-4 exhibited different morphology, as shown in Fig. 2(b), due to the irregular surface left on the Zircaloy-4 sample by the deformation of the substrate by the glass beads particles during grit blasting.

The only sample which exhibited any evidence of cracks in the SiC film surfaces, was the pre-oxidized

Table 2
Roughness of all samples surfaces of Group B before and after coating

Sample	Roughness, R_a (nm)	
	Substrate	After coating (1 μm)
A. As-received	220	340
B. 600 grit	310	380
C. 240 grit	950	500
D. 240 grit and pickled	950	590
E. Grit blasted	2520	2320
F. Pre-oxidized	310	720
H. Carbon interlayer	310	470

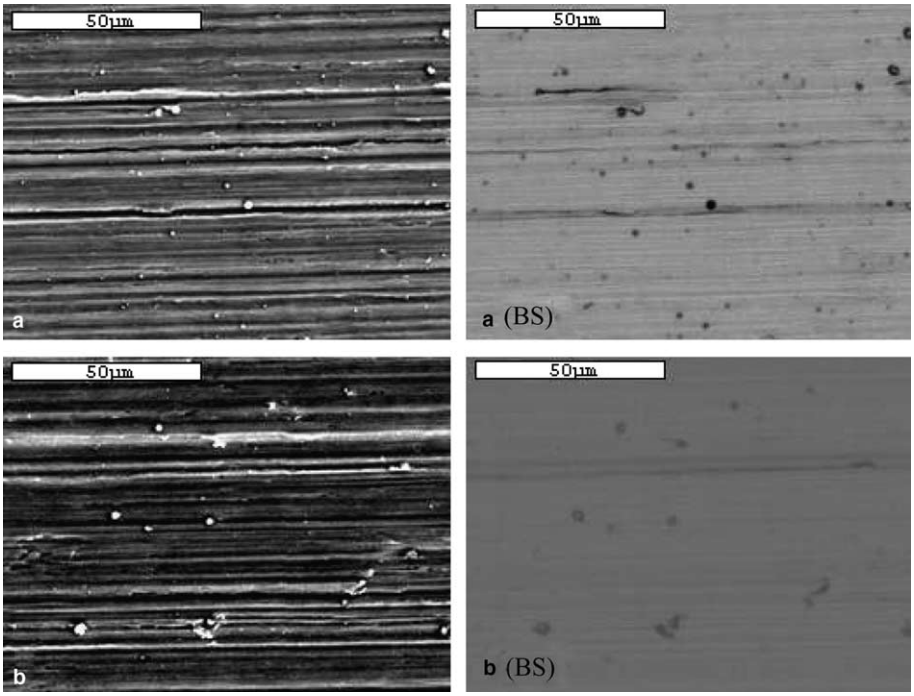

Fig. 1. Typical secondary electrons and backscattered (BS) images of a coated surface on (a) 600 grit polished substrate, (b) 240 grit polished substrate.

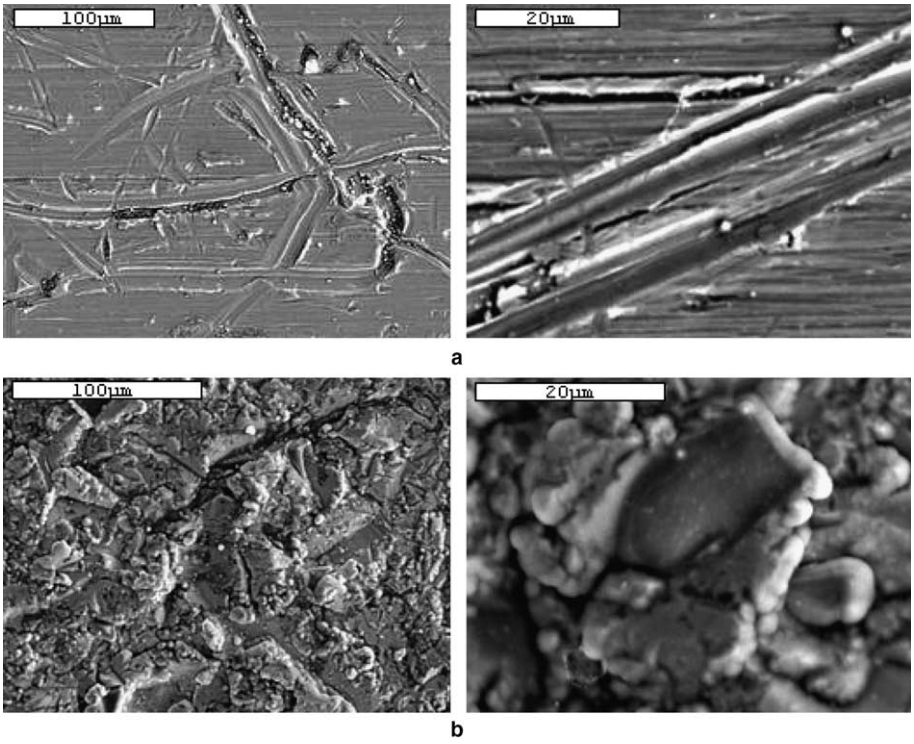

Fig. 2. Low and high magnification SEM image of the top surface of the SiC films (a) deposited on the as-received Zircaloy-4 sample, (b) deposited on grit blasted (high roughness) Zircaloy-4 substrate sample.

substrate sample, as shown in Fig. 3(a)–(c). The cracks in the SiC film appeared to form due to the formation of cracks and spallation of the approximately 100 μm thick brittle oxide film formed on the Zircaloy substrate during the pre-oxidation treatment. Cross-sectioned SEM images of oxide/substrate interfaces are shown in Fig. 3(d)–(f). As expected, the thick oxide layer was formed due to the high oxidation temperature, 1200 °C, which lead to the formation of the thick ZrO_2 surface oxide film. No cracks were observed to propagate through the oxide layer, and most of the cracks were found along the interface as shown in Fig. 3(d). However, some cracks were found to propagate in a region between the oxide film and Zircaloy metal (Fig. 3(e) and (f)) which could be caused by an embrittlement of the zirconium metal at the metal/oxide interface by oxygen.

Chemical analysis of the top surface of the SiC coatings on all coated samples, regardless of film thickness or surface preparation, showed similar EDS profiles, as shown in Fig. 4. Chlorine peaks were found in all samples and is thought that this may be detrimental to the corrosion resistance of SiC films [28].

A scratch test was made on all samples. The average critical load was obtained by generating 3–5 scratches, 3 mm long, for each sample, as shown in Fig. 5. During

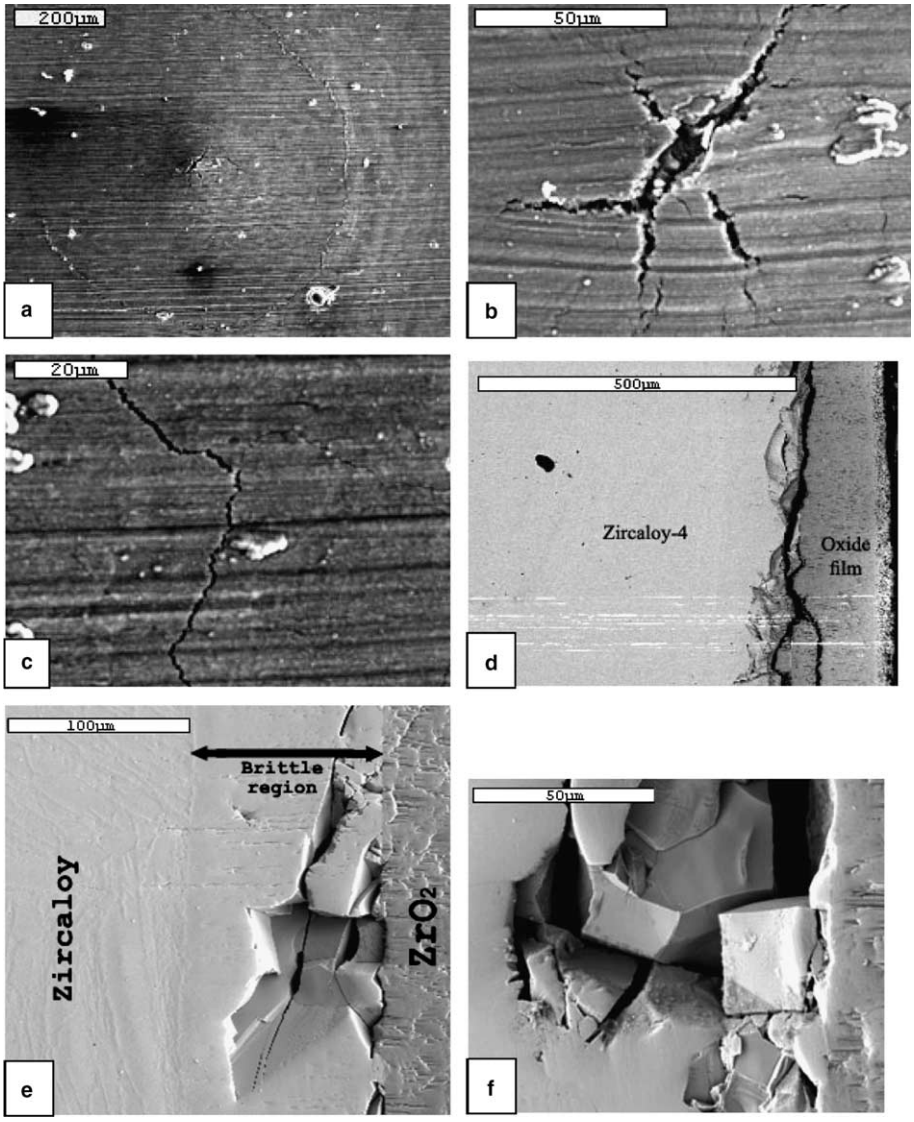

Fig. 3. SEM images show the thickness and cracks on the oxide film of Zircaloy-4 oxidized at 1200 °C (a)–(c) top surface, (d)–(f) cross section.

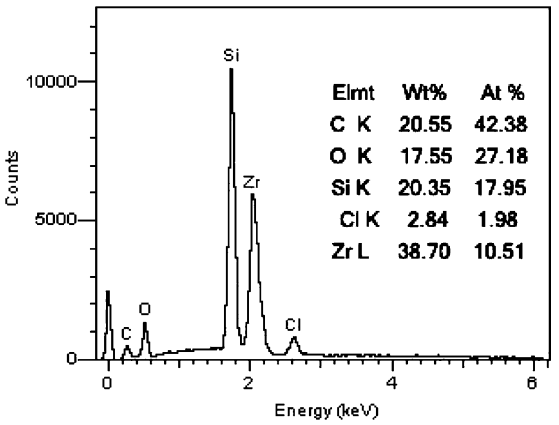

Fig. 4. Typical EDS spectrum of top surface of Zircaloy-4 coated with 1 μm thick SiC film of group B samples.

testing, the applied normal force, the tangential force and the acoustic emission (AE) signal intensity were recorded. Fig. 6(a) shows a typical graph obtained from one of the scratch tests. The critical load is taken at the point where there is a change in the friction between the stylus and the surface. Fig. 6(b) illustrated the good agreement that was obtained between the results from tangential force measurements and acoustic emission detection in the determination of critical load.

The scratch tracks, as examined by SEM, were composed of three stages with an increase in the applied loads. The first stage, at low applied load, involved plastic deformation of the film and the substrate, which caused some flaking of the film around the scratch line. The second stage indicated the appearance of cracks and detachment of small pieces ahead of the scratch stylus. The third stage, which starts at the critical load, contains continued delamination of the film ahead of the scratch stylus. SEM was also used to determine the type of failure that occurred. Cohesive failure was observed to occur within the coating; whereas, an adhesive failure occurred at the interface of the coating–substrate system.

Adhesive failure was observed on all sample, as shown in back-scattered SEM images and confirmed by EDS analysis of scratch channels (Fig. 7). Fig. 8 shows the morphology of scratch tracks on SiC film tested in the low load regime, before the start of continuous delamination. Detachment and spallation of the film around the scratch tracks were observed. The coating was removed due to the plastic deformation of the film and/or substrate rather than direct contact with stylus. This type of delamination is a typical event for the adhesive mode of failure when the film tends to flake away or de-bond at the edges of scratch channel.

The critical force, L_c, for each samples at which damage of the coating occurs is given in Fig. 9. The pre-oxidized sample did not show any clear delamination of the film up to loads approaching more than 30 N. The graph shows a higher adhesion strength for 240 grit finish compared to the other finer and rougher surfaces (600 grit and the grit blasted samples) respectively. Fig. 10 shows the variation of the critical load as a function of the coating surface roughness. Higher adhesion strengths were observed at a moderate level of substrate roughness. Coating on pickled substrate shows higher critical loads than when only ultrasonically cleaned. The samples with sputtered carbon interlayer did not show any noticeable improvement in the adhesion of the SiC coating on the Zircaloy-4.

The higher critical loads were found in samples with intermediate values of substrate surface roughness. Scratch tests showed that a smooth substrate, such as, a 600 grit polish, induces a relatively poor adhesion strength compared to a rough 240 grit polish substrate. This decrease in adhesion with increasing surface smoothness was attributed to the larger contact surface and possibly by mechanical 'interlocking' [10] between film/substrate caused by roughening of the substrate. However, it is important to mention that the increase in the roughness of the film above the 240 grit surfaces lead to a decrease in the critical load due to an increase in the coefficient of friction during the scratch test [29]. The increased coefficient of friction increased the

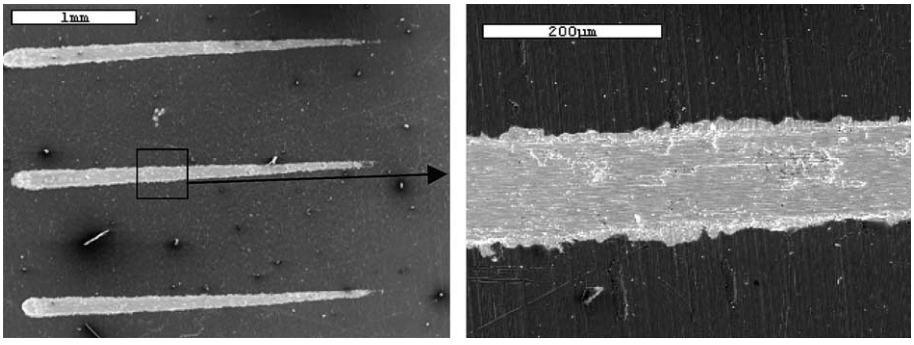

Fig. 5. SEM micrographs of the scratch channels on the 1 μm SiC film on Zircaloy.

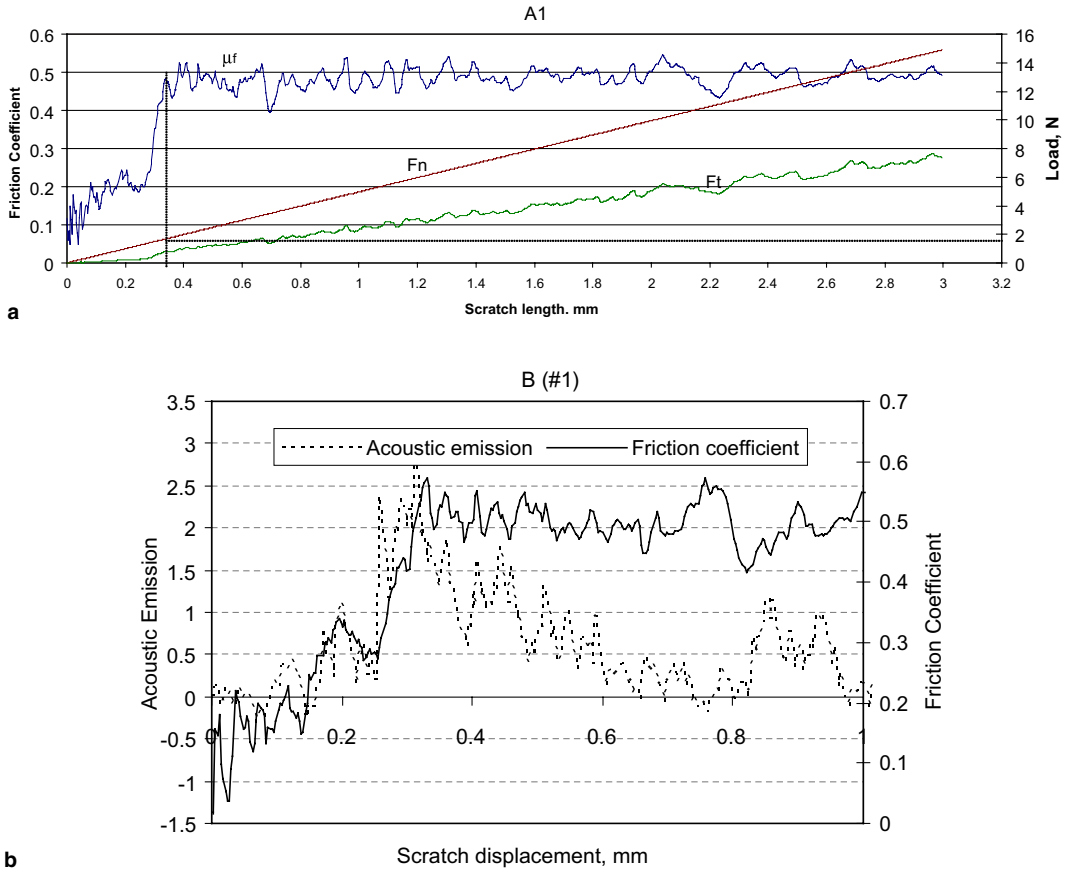

Fig. 6. Typical graphs of scratch test show (a) variation of normal force and tangential force as function of scratch length, (b) good agreement between friction measurement and acoustic emission detection in the scratch test.

tangential forces and hence the shear stresses available for film detachment. This may explain the lower values of critical load found in the very rough (grit blasted) samples compared to the smoother, 240 grit, surface. Substrate surface cleanliness before coating showed a significant increase in the adhesion between film and substrate (Fig. 9). Increased adhesion from increased cleanliness of the substrate was believed to be due to remove all impurities and oxides particles from the surface which, if present between film and substrate, would act as an initiation site for cracks at the interface. These results were consistent with previous reports that indicated [30,31] that better adhesion was observed in samples with increase cleanliness (see, for example Fig. 11).

Pre-oxidation of the Zircaloy substrate at high temperature, 1200 °C produced a very thick oxide layer with intensive cracking at the interface. Cracks at the interface were attributed to the high compressive residual stresses generated in the film during the transformation from Zr to ZrO_2 with a dramatic volume increase since the volume dilatation due to the oxide formation is approximately 1.5. Because ZrO_2 has very high fracture toughness, no cracks were observed to propagate through the oxide layer, and most of the cracks were found along the interface as shown in Fig. 3(d). The fracture toughness for zirconia is approximately 12 MPa $m^{1/2}$ which is twice of that reported for SiC [32].

Since the load during scratch testing increased to 15 N over the relatively short length of the scratch (i.e., 3 mm), there can be a tendency to push small areas of removed material and flaws ahead of the stylus. The resulting build up of material ahead of the stylus can produce loads that appear greater than were required to initiate the removal of the coating. Although the critical loads for coating delamination were much lower than the maximum load of 15 N, which tends to lessen the concern regarding the potential for artificially high levels of apparent measured loads, a few tests at lower loads were used to verify the measured loads for coating failure. Therefore, samples of the as-received, 240 grit surface finish and 600 grit surface finish were tested at a lower load (3 N) using a finer stylus (20 μm). The results of the tests at lower loads were very similar to the results of testing at higher loads. The critical loads

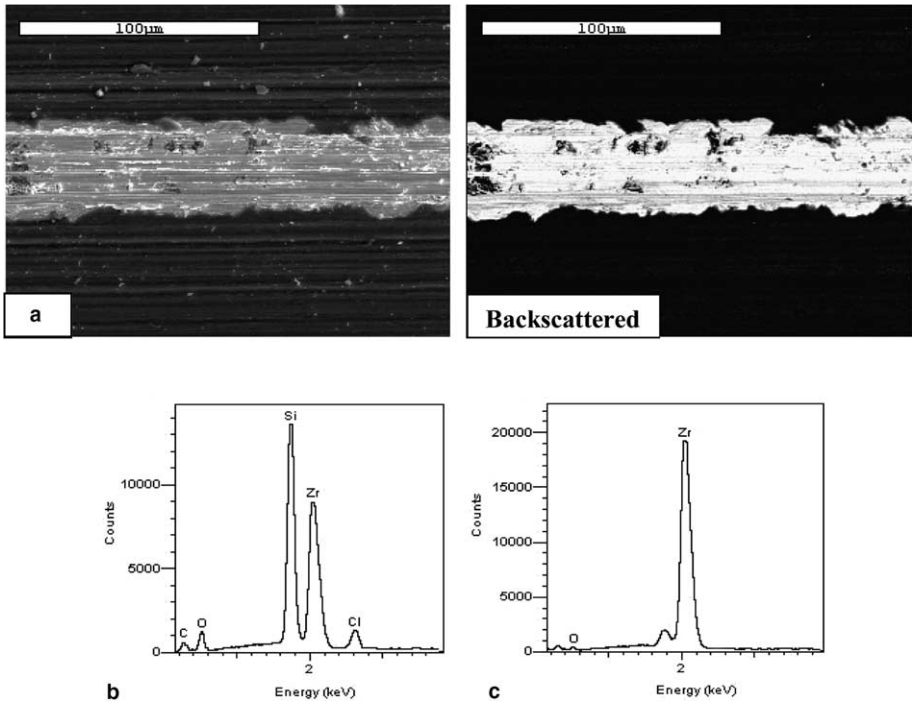

Fig. 7. Coated sample after scratch test shows adhesive failure of (a) SEM SE and BS images of scratch track, (b) EDS spectrum from coated area, (c) EDS spectrum inside scratch track.

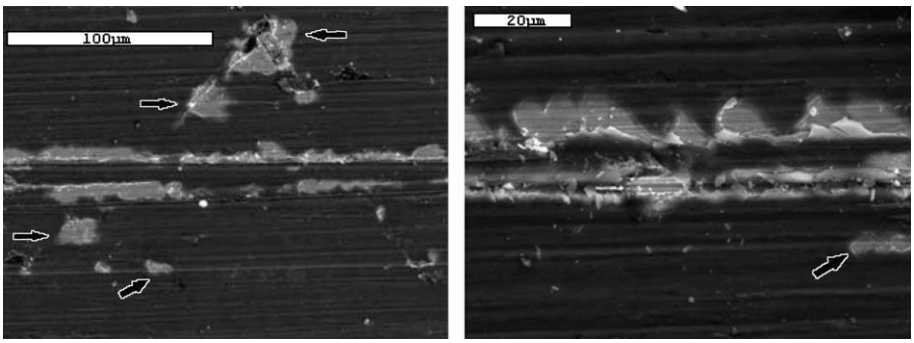

Fig. 8. SEM images of SiC coatings show detachment of the film around the stylus track.

for all three conditions were in the 1.5–2.0 N range, with the highest load observed in the sample with 240 grit surface finish (2.0 N). The samples with the as-received and the 600 grit surface finish exhibited slightly lower critical loads, 1.5 N and 1.7 N, respectively.

4. Corrosion protection

Impedance measurements were carried out to investigate the effect of the surface treatments and adhesion strength on the corrosion protective properties of the SiC coating. Fig. 12 shows the EIS spectra of the uncoated and SiC coated samples in a HF 0.001 M/HCl 1 M/HNO_3 1 M solution. The low frequency impedance amplitude, $|Z|$, of the Zircaloy-4 substrate was remarkably enhanced after SiC deposition, which showed the excellent corrosion protective properties of the PACVD SiC hard film.

The $|Z|$ of the SiC film on 240 grit surface finished Zircaloy-4 was slightly higher than SiC film on 600 grit surface finished Zircaloy-4. This suggests that the higher adhesion strength provides better corrosion protective performance of coated system [27]. Although, the inter-

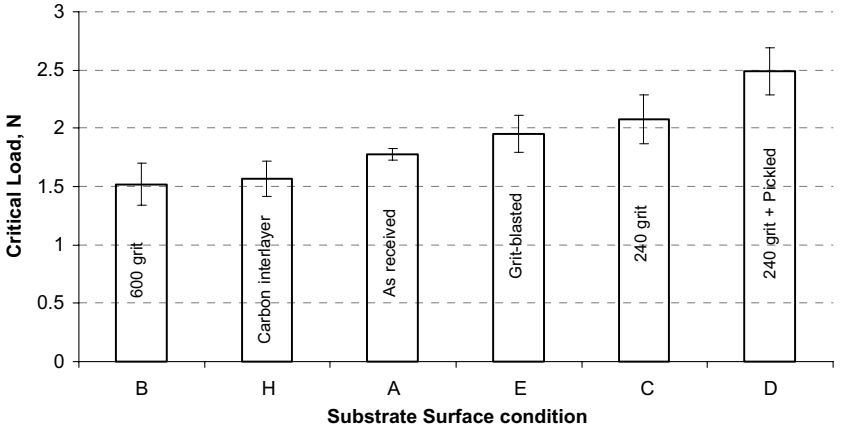

Fig. 9. Critical load of SiC coating failure as a function of substrate surface preparation.

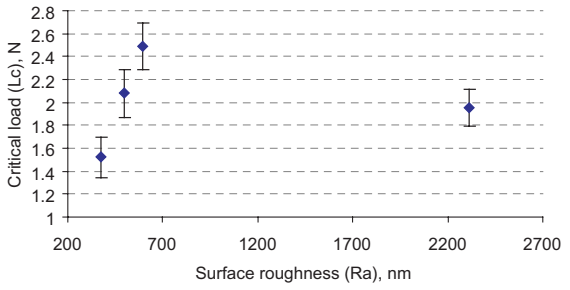

Fig. 10. The variation of critical load with coating surface roughness.

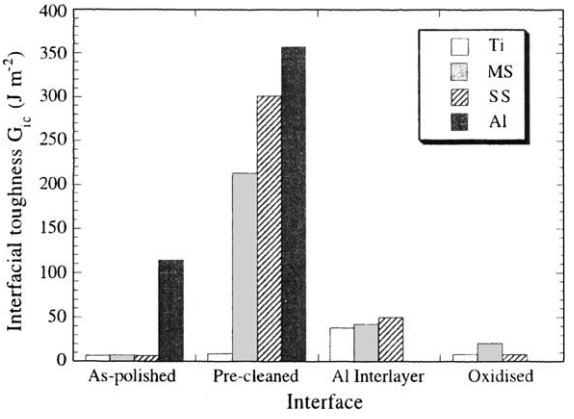

Fig. 11. Experimental data shows the effect of pre-cleaning on the interfacial toughness of DLC coatings deposited on different substrates [31].

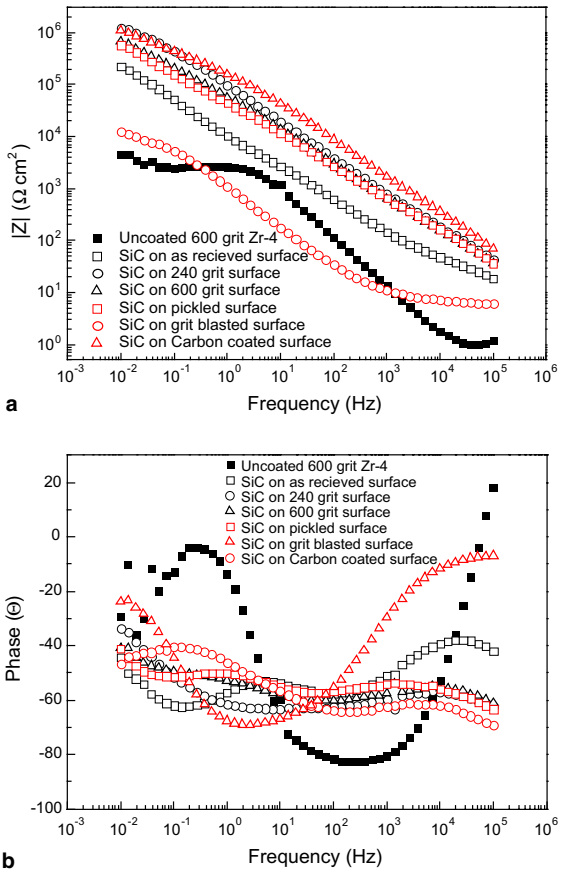

Fig. 12. Impedance spectra for the uncoated and SiC coated Zircaloy-4 substrates in HF 0.001 M/HCl 1 M/HNO_3 1 M mixture. (a) Bode magnitude, (b) bode phase plots

mediate critical load was measured from scratch test, the grit blasted sample showed the lowest $|Z|$ attributed to the extremely high surface roughness. This rough surface, Fig. 13, increased the tendency for coating defects to form, in spite of strong mechanical 'interlocking' between coating and substrate. In the same way, a relatively lower $|Z|$ was observed on samples with a SiC

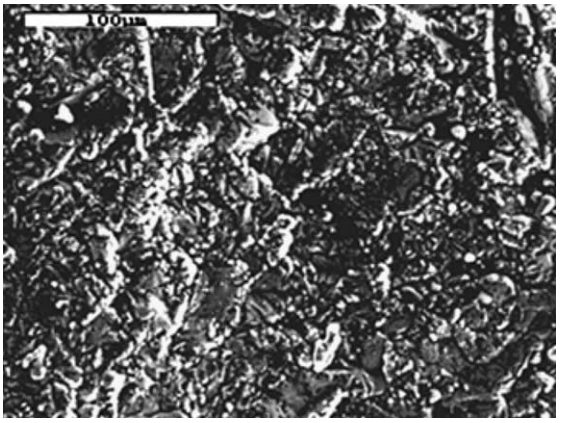

Fig. 13. SEM image of the grit-blasted Zircaloy-4 surface coated with 1 μm SiC after EIS test in HF 0.001 M/HCl 1 M/HNO_3 1 M mixture.

coating on the as-received surface. This could also be produced by the localized defect density or non-uniformity of the substrate, such as large cracks, on the substrate [10,11]. Ulrich, et al., reported that the highest $|Z|$ obtained from carbon deposited samples was due to the introduction of an interlayer and/or multilayer to enhance the corrosion performance of the hard coating [9]. They suggested that this effect was based on the reduction of through-coating porosity or defect by adding interfaces to the coating structure, and by increasing thickness. Two mechanisms have been used to explain the correlation of corrosion resistance of a ceramic coating with its thickness. The two mechanisms are: (a) coating microstructure, and (b) diffusion processes of corrosive media [7,8]. An increase in the free energy for the generation of an active defect was observed as the coating thickness increased. Therefore, increasing the thickness of coatings can greatly reduce the number of permeable defects. Second, compared to diffusion occurring in the large volume of solution, the key step controlling the corrosion reaction at the coating/substrate interface is the diffusion or mass migration confined within the pores. Increasing coating thickness extends the pore length, so that diffusion restricted in the small pore is much more difficult [8]. The pickled sample did not display the highest corrosion resistance, although it did exhibit the highest critical load during adhesion testing. This showed that the native zirconium-oxide interlayer (ZrO_2) also enhances the corrosion protective performance of SiC coatings.

5. Conclusions

Scratch testing can give useful information regarding the adhesion of coatings provided that careful understanding of the failure modes and interpretation of the results and scratch morphologies is carried out. The results indicate that the roughness morphology may affect the adhesion strength of the PACVD SiC coatings. Higher adhesion values were found at the intermediate level of roughness. Furthermore, cleanliness of the substrate improved the adhesion.

The corrosion resistance of these films was closely related to the measured adhesion between the film and the substrate. The strong adhesion of SiC film on rough surfaces of the Zircaloy-4 substrate surfaces, resulted in higher corrosion resistance.

Acknowledgement

This work was supported by DOE funded NERI contract, DE-FG03-99SF21882.

References

[1] R. Baney, J. Tulenko, R. Singh, G.E. Fuchs, D. Butt, P. Demkowicz, P. Schoessow, G. Park, J. Kim, Y. Al-Olayyan, S. Bang, in: P. Vincenzi (Ed.), Proceedings from CIMTEC (International Conference on Modern Materials and Technologies), Faenza, Italy, Techna, 2003, p. 181.
[2] H. Stone, T. Kaneko, N. Miyakawa, J. Cryst. Growth 219 (2000) 245.
[3] J. Hofmann, S. Veprek, Thin Solid Films 318 (1998) 18.
[4] S.J. Toal, H.S. Reehal, S.J. Webb, N. Barradas, C. Jeynes, Thin Solid Films 343–344 (1999) 292.
[5] G. Foti, Appl. Surf. Sci. 184 (2001) 20.
[6] D. Lespiaux, F. Langlais, R. Naslain, S. Schamm, J. Sevely, J. Europ. Ceram. Soc. 15 (1995) 81.
[7] C. Liu, A. Leyland, Q. Bi, A. Matthews, Surf. Coat. Technol. 141 (2001) 164.
[8] C. Liu, Q. Bi, A. Leyland, A. Matthews, J. Vac. Sci. Technol. 20 (2002) 772.
[9] R.K. Ulrich, D. Yi, W.D. Brown, S.S. Ang, Thin Solid Films 209 (1992) 73.
[10] R.K. Ulrich, D. Yi, W.D. Brown, S.S. Ang, Corros. Sci. 33 (1992) 403.
[11] L.H. Hihara, A. Iwane, S. Voss, R.E. Rocheleau, Z. Zhang, Corros. Sci. 41 (1999) 1403.
[12] S. Amada, T. Hirose, Surf. Coat. Technol. 102 (1998) 132.
[13] Z. Xie, J. Zhu, W. Guo, Mater. Charact. 44 (2000) 347.
[14] J. Valli, U. Makela, J. Vac. Sci. Technol. A3 (6) (1985) 2411.
[15] J.E. Pawel, C. Hargue, Adhes. Measure. Films Coat. (1995) 323.
[16] D. Wang, M. Chiu, Surf. Coat. Technol. 156 (2002) 201.
[17] K. Walter, M. Nastasi, C. Munson, Surf. Coat. Technol. 93 (1997) 287.
[18] C. Chang, D. Wang, Nucl. Instr. Meth. Phys. Res. B 194 (2002) 463.
[19] B. Liu, B. Jiang, Y. Fu, D. Cheng, X. Wu, S. Yang, Thin Solid Films 349 (1999).
[20] A. Pan, J.E. Greene, Thin Solid Films 97 (1982) 79.

[21] M. Andrieux, M. Ducarroir, E. Beaurprez, Thin Solid Films 324 (1998) 141.
[22] F.S. Shieu, R. Raj, S.L. Sass, Acta Met. Mater. 38 (11) (1990) 2215.
[23] G.W. Critchlow, J. Hampshire, R. Kingdon, Z. Naeem, A.B. Smith, D.G. Teer, Tribol. Int. 30 (7) (1997) 499.
[24] B. Ollivier, A. Matthews, Adhes. Measure. Films Coat. (1995) 103.
[25] A. Perry, Thin Solid Films 78 (1981) 77.
[26] A. Perry, Thin Solid Films 81 (1981) 357.
[27] S.C. Lee, F.D. Lai, W.Y. Ho, Chem. Phys. 43 (3) (1996) 266.
[28] Y.G. Gogotsi, S. Welz, J. Daghfal, M.J. McNallan, I.D. Jeon, K.G. Nickel, T. Kraft, Ceram. Eng. Sci. Proc. 19 (3) (1998) 87.
[29] S.J. Bull, Wear 233–235 (1999) 412.
[30] P. Benjamin, C. Weaver, Proc. Roy. Soc. London A254 (1960) 163.
[31] T. Fukushima, S. Kuroda, S. Kitahara, Vacuum 41 (4–6) (1990) 1297.
[32] J.R. Davis, Structural ceramics, in: ASM Specialty Handbook on Heat Resistant Materials, Materials Park, OH, 1997, p. 415.